Chinese Journal of Aeronautics 24 (2011) 81-89

Contents lists available at ScienceDirect

Chinese Journal of Aeronautics

journal homepage: www.elsevier.com/locate/cja

Control-oriented Modeling for Air-breathing Hypersonic Vehicle Using Parameterized Configuration Approach

LI Huifeng*, LIN Ping, XU Dajun

School of Astronautics, Beijing University of Aeronautics and Astronautics, Beijing 100191, China

Received 21 April 2010; revised 12 June 2010; accepted 30 August 2010

Abstract

This article presents a parameterized configuration modeling approach to develop a 6 degrees of freedom (DOF) rigid-body model for air-breathing hypersonic vehicle (AHV). The modeling process involves the parameterized configuration design, inviscous hypersonic aerodynamic force calculation and scramjet engine modeling. The parameters are designed for airframe-propulsion integration configuration, the aerodynamic force calculation is based on engineering experimental methods, and the engine model is acquired from gas dynamics and quasi-one dimensional combustor calculations. Multivariate fitting is used to obtain analytical equations for aerodynamic force and thrust. Furthermore, the fitting accuracy is evaluated by relative error (RE). Trim results show that the model can be applied to the investigation of control method for AHV during the cruise phase. The modeling process integrates several disciplines such as configuration design, aerodynamic calculation, scramjet modeling and control method. Therefore the modeling method makes it possible to conduct AHV aerodynamics/propulsion/control integration design.

Keywords: flight dynamics; hypersonic; AHV model; parameterized configuration design; aerodynamics/propulsion integration

1. Introduction

With a large altitude-velocity flight envelope, wild-varying disturbances and complicated environment, the near space hypersonic vehicle becomes strong coupling, fast time-varying, highly nonlinear and great uncertain. Integration of attitude control, engine thrust regulation and guidance control are required[1]. Therefore, the development of reasonable air-breathing hypersonic vehicle (AHV) model is inevitable.

Two models are widely used for hypersonic control research. One is winged-cone model developed by NASA Langley Research Center and opened to public in 1990 (that is generic hypersonic vehicle (GHV) model). This model aims to develop a manned, horizontal takeoff and landing, single-stage-to-orbit (SSTO), air-breathing launch vehicle. It covers a large operational range from subsonic to hypersonic, and the aerodynamic data is sophisticated from both wind tunnel tests and aerodynamic preliminary analysis system (APAS). This mathematical model is applied to reducing the vehicle trim drag force, developing the guidance and control strategies and evaluating the vehicle performances[2-5].

The other one is air-breathing hypersonic flight vehicle (AHFV), which is a two-dimensional vertical model based on gas dynamics and computational fluid dynamics (CFD). AHFV is used by Multidisciplinary Flight Dynamics and Control Laboratory at California State University, Los Angeles (CSULA), to research aerodynamics/propulsion coupling effect and control methodology, also known as CSULA-GHV model[6-9]. The widely used 3 degrees of freedom (DOF) (plus flexibility) nonlinear model for the longitudinal dy-

*Corresponding author. Tel.: +86-10-82339276.
E-mail address: lihuifeng@buaa.edu.cn
Foundation item: Aeronautical Science Foundation of China (2008ZA51002)

doi: 10.1016/S1000-9361(11)60010-1

namics of a generic scramjet hypersonic vehicle is also utilized by Bolender, et al.[10-14].

However, the winged-cone model does not have aerodynamics/propulsion integration configuration, which is a general characteristic for hypersonic wave rider. Only the effect of hypersonic velocity is reflected in the dynamic equations. Although the 6 DOF model has been developed, it is usually reduced to longitudinal model for control algorithms study. The CSULA-GHV model emphasizes the aerodynamics/propulsion integration design, but the model is limited in vertical plane which is mainly used for scramjet modeling research and only simple control method is discussed.

Besides, with fixed configuration, existing models cannot reflect interaction between aerodynamic profile and propulsion performance, so they cannot be used to conduct research on aerodynamics/propulsion/control integration. Therefore, we present a method to develop 6 DOF rigid-body model for AHV using parameterized configuration approach. Trim calculation results show that AHV model can be applied to the control algorithm research for AHV during the cruise phase. The modeling process integrates several disciplines such as configuration design, aerodynamic calculation, scramjet modeling and control method. Therefore the modeling method makes it possible to conduct AHV aerodynamics/propulsion/control integration design. In addition, some advanced control actuator (vector control, direct force control and variable centroid control, etc.) can also be introduced into the modeling process, so it is flexible to explore and verify varieties of control methods for AHV.

The modeling procedure for AHV is as follow. After selecting the general parameters and flight conditions for target vehicle, the aircraft aerodynamic profile and engine shape are obtained through parameterized design. Then, the aerodynamics/propulsion data is calculated by inviscous hypersonic aerodynamic force calculation and the quasi-one dimensional combustor calculation. Finally, the model is verified by trim calculation.

2. Parameterized Configuration Design

For AHV, the magnitude of thrust is at the same order with drag force. In order to reduce the drag and obtain the thrust as large as possible, the highly integrated aerodynamics/propulsion system is required. With integrated design, the incoming flow can be pre-compressed by the forebody before getting into the engine inlet. The afterbody plays a role as an "outside nozzle" to enable further expansion of burned propellants. The high temperature gas stream pressed on the undersurface of the afterbody causes further lift which has great impact on aerodynamic performance of AHV[15].

Parameterized configuration approach determines the geometric configuration of AHV by setting a series of parameters. Table 1 lists some parameters. With these parameters, the PLOT3D format data file is generated by self-developed geometric configuration program. AHV 3D profile is shown in Fig.1. Configuration modification can be achieved easily through resetting corresponding parameters in the program. For the models from CFD software, it is inevitable to re-mesh the vehicle and flow field. The presented method could avoid these troubles which brings a great convenience at the conceptual stage of AHV design. What's more, this allows us to utilize the multidisciplinary design optimization (MDO) methods which can combine AHV aerodynamics and propulsion design to get the best overall performance.

Table 1 Configuration parameters of AHV (partly)

System	Variable symbol	Value	Meaning
Airframe	L_body	4.27 m	Body length
	W_body	0.584 2 m	Body width
	H_upsurface	0.2 m	Body height
	W_engine	0.4 m	Engine width
	y_engine	−0.4 m	Longitudinal coordinate of engine bottom
Airframe/Engine integration	delta1_forebody	5°	First wedge inclination of forebody
	delta2_forebody	10°	Second wedge inclination of forebody
	x1_forebody	0.2	Axial relative coordinate of intersection of wedge 1 and wedge 2
	x2_forebody	0.4	Axial relative coordinate of intersection of wedge 2 and scramjet engine
	x_nozzle	0.75	Axial relative coordinate of intersection of scramjet engine and afterbody
	delta_outernozzle	11°	Inclination of outside part of afterbody
	x1_engine	0.35	Axial relative coordinate of the front point of engine bottom
	x2_engine	0.8	Axial relative coordinate of the rear point of engine bottom
Wings	L_wingroot	0.94 m	Chord length of wing root
	L_wingtip	0.558 9 m	Chord length of wing tip
	L_wingspan	0.33 m	Wing length
	theta_sweepback	45°	Sweep angle of leading edge
	c_wingthickness	0.02	Relative thickness

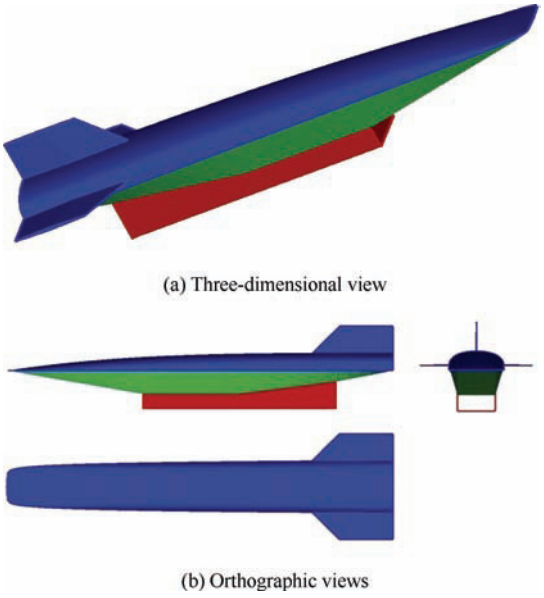

(a) Three-dimensional view

(b) Orthographic views

Fig.1 Effect pictures of AHV.

3. General Parameters and Flight Conditions

The general parameters and flight conditions of AHV should be determined before aerodynamic and thrust calculation. A few parameters can be obtained from the similar vehicle[16], but most of them need to be reassigned through times of iterations based on the mission object function from initially estimated values. The results are shown in Table 2.

Table 2 General parameters of AHV

Variable symbol	Value	Meaning
m	671.33 kg	Mass of AHV
S	0.298 6 m^2	Reference area
c_A	0.373 2 m	Reference length (mean aerodynamic chord)
b_A	0.8 m	Lateral reference length
I_x	34.13 kg·m^2	Moment of inertia around x axis
I_y	1 040 kg·m^2	Moment of inertia around y axis
I_z	1 034 kg·m^2	Moment of inertia around z axis
I_{xz}	430.0 kg·m^2	Product of inertia

The setting of flight conditions decides the flight envelope which is critical to the calculation of aerodynamics/propulsion.

AHV model is mainly established for guidance and control investigation during the cruise phase. The magnitude of angle of attack (AOA) is limited within a typical range, and so are the altitude and velocity. On the other hand, because AHV has aerodynamics/propulsion integration configuration, the bank to turn (BTT) control technology has to be adopted. Thus the sideslip angle magnitude is constrained within permitted threshold. Table 3 gives the resultant flight conditions.

Table 3 Flight conditions of AHV

Variable symbol	Value	Meaning
H	25-35 km	Height
Ma	5-7	Mach number
α	−2°-10°	Angle of attack
β	−6°-6°	Angle of sideslip
δ_{e1}, δ_{e2}	−20°-20°	Deflection angles of left and right wings
δ_r	−10°-10°	Deflection angle of vertical tail

4. Aerodynamics and Propulsion Modeling

4.1. Partitioning of aerodynamic force and thrust

The areodynamics/propulsion integration configuration brings strong couplings between aerodynamics and propulsion system. To understand their interaction better, it is necessary to partition aerodynamic force and thrust. AHV is divided into aerodynamics system and propulsion system. Both of them are partitioned with the approach in Ref.[9]. The details are shown in Fig.2. The aerodynamics system includes forebody, external compression part of inlet, wings, empennage, the upper surface and side surface of the vehicle, the cowl of the engine. The propulsion system includes the flow passage inside the engine and the nozzle.

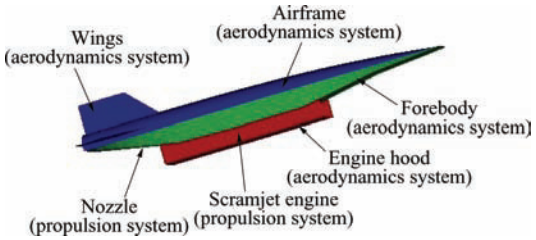

Fig.2 Partitioning of aerodynamic force and thrust.

4.2. Inviscid hypersonic aerodynamics calculation

During conceptual design period, proper prediction of aerodynamic performance is of great importance because wind tunnel tests are highly time- and money-consuming. The CFD software such as Fluent is commonly used in the calculation of hypersonic aerodynamics because of its high precision. But it is still time-consuming and not suitable for exploratory design research of AHV. Even the geometric configuration parameters change slightly, the aircraft has to be re-drawn, so a simpler and more effective approximate aerodynamic calculation method is in need.

During the hypersonic flight, most aerodynamic force comes from inviscid hypersonic flow. Particularly, aerodynamic force and moment could be predicted through inviscid flow analysis. This method could be applied in parameterized modeling to reduce the modeling period.

Different methods are used to estimate the pressure coefficient for airframe and wings, according to the

situations of the windward sides and the leeward sides. Considering the missions, flight environment and vehicle configuration, this article adopts the Dahlem-Buck method for the windward sides of airframe, and the Prandtl-Meyer method for the leeward sides of airframe. The cone method and expansion-wave method are used for windward and leeward sides for wings respectively[17]. Parts of the results are shown in Figs.3-4.

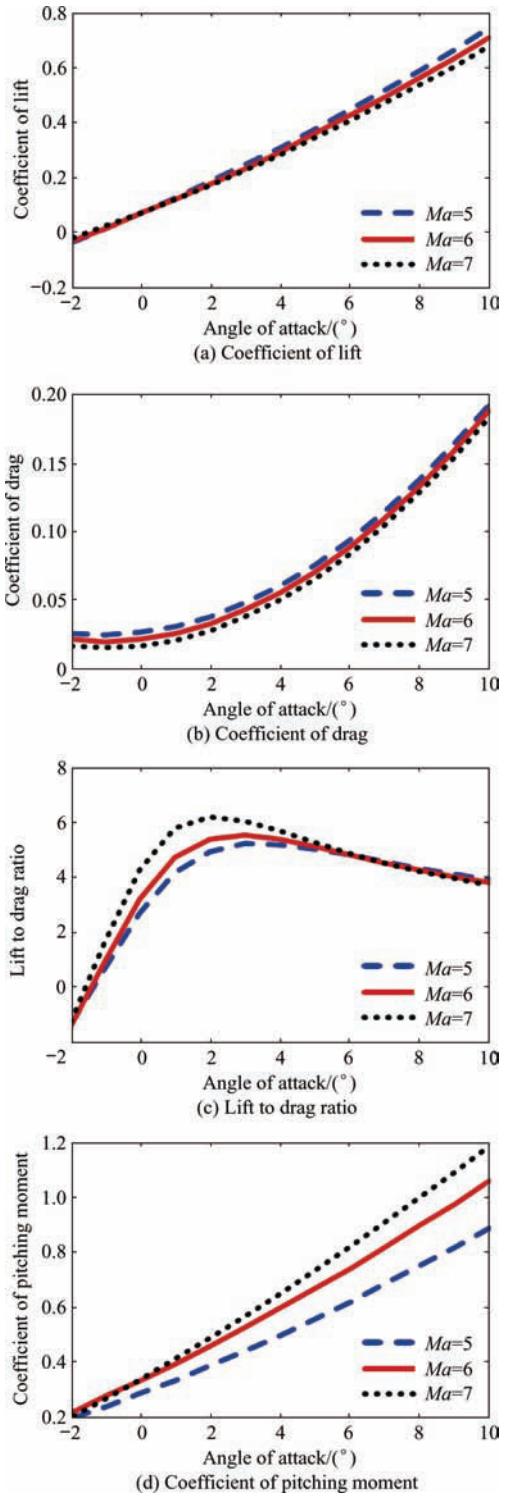

Fig.3 Longitudinal aerodynamic characteristics of AHV.

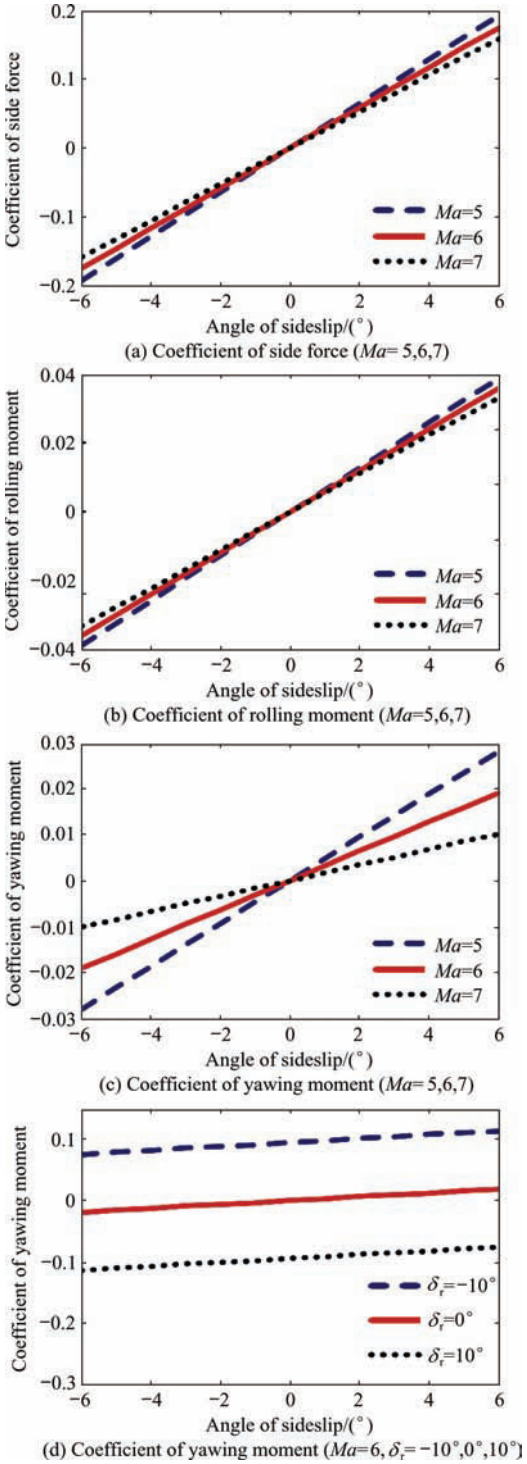

Fig.4 Lateral aerodynamic characteristics of AHV.

As depicted from the above figures, aerodynamic characteristics of this AHV have the following features:

The longitudinal static stability derivative $\partial C_m/\partial\alpha$ is larger than 0, demonstrating that the longitudinal mode of AHV is statically instable; the dihedral derivative $\partial C_l/\partial\beta$ is also larger than 0, which means that the rolling mode of AHV is statically instable; the yawing stability derivative $\partial C_n/\partial\beta$ is larger than 0, indicating that the yawing mode of AHV is statically stable. The

lift to drag ratio is relatively high, which means AHV has good aerodynamic efficiency.

4.3. Scramjet engine modeling

There are two parts related to the thrust of AHV, airframe's lower surface and engine hood, as shown in Fig.5. The lower surface is divided into forebody, middle part and afterbody. The scramjet engine is composed of the middle part and the engine hood. The details of each and corresponding functions are shown in Table 4, and some of the results of thrust calculation are shown in Fig.6.

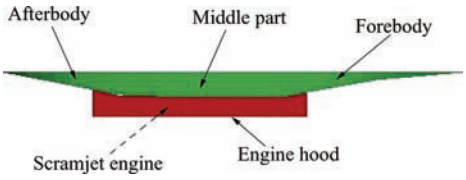

Fig.5 Parts related to thrust: lower surface and engine.

Table 4 Mechanism of thrust of AHV

Section	Position	Function	Theories involved
Forebody/Inlet	Front part of lower surface	Pre-compress inflow (1) To reduce the inflow Mach number and lower the burning difficulty. (2) To increase pressure and improve combustion efficiency.	Oblique shock wave theory, expansion wave theory, inviscid hypersonic aerodynamics calculation
Scramjet engine	Middle part of lower surface and engine hood	Supersonic combustion (1) To control the thrust through fuel equivalence ratio δ_T. (2) To produce the uninstalled thrust.	Quasi-one dimensional combustor theory[18]
Afterbody/Nozzle	Rear part of lower surface	Expand wake flow (1) To produce the thrust, aerodynamic forces and moments. (2) To produce expansion wave, increase the Mach number, reduce the pressure to make the pressure of wake flow be equal to the external pressure.	Expansion wave theory

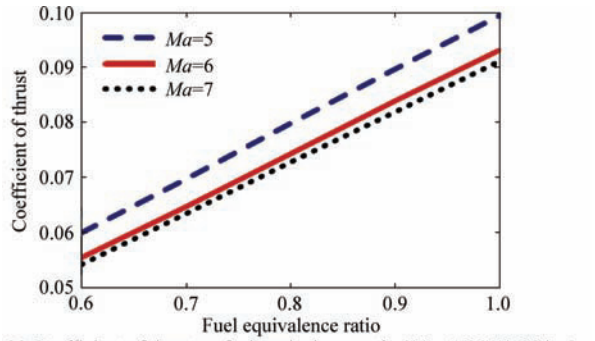

(a) Coefficient of thrust vs fuel equivalence ratio (Ma=5,6,7,H=30 km)

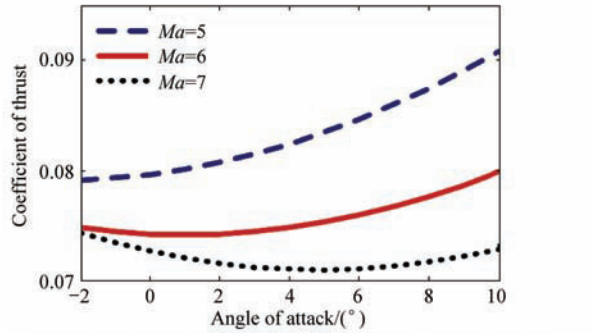

(b) Coefficient of thrust vs angle of attack (Ma=5,6,7,H=30 km)

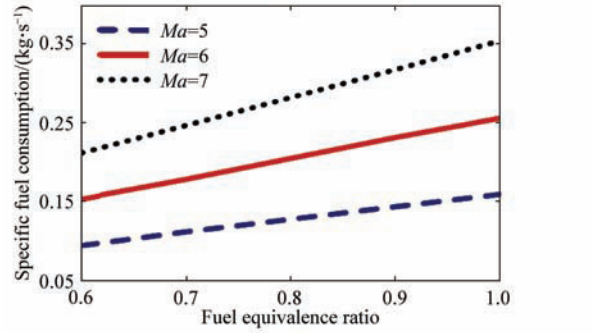

(c) Specific fuel consumption vs fuel equivalence ratio (Ma=5,6,7,H=30 km)

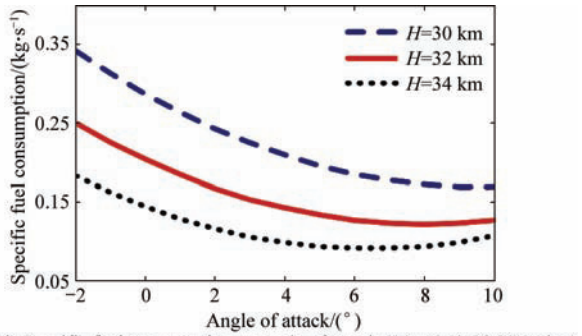

(d) Specific fuel consumption vs angle of attack (Ma=6,H=30,32,34 km)

Fig.6 Engine characteristics of AHV.

After analyzing the preceding calculation results, the following conclusions are obtained.

(1) The thrust of AHV consists of two parts, one is the uninstalled thrust from the scramjet engine, which is yielded according to the momentum conservation law between the vehicle and high speed exhaust ejecting from the nozzle; the other part is the vector sum of the pressure generated by the high temperature exhaust on the surface of vehicle afterbody, and this is calculated with Prandtl-Meyer formula. Generally speaking, the thrust generated from the afterbody is larger than the uninstalled thrust. And the afterbody contributes about 60% to 80% of the total thrust.

(2) The states before and after the shock wave are calculated by the oblique shock wave theory, and the results are served as the interface conditions of scramjet engine. The forebody only generates aerodynamic force which is predicted by the inviscous hypersonic aerodynamic theory, as shown in Fig.2.

(3) The resultant data shows that exhaust flow state, uninstalled thrust and specific fuel ratio are all influ-

enced by the states after the oblique shock wave and the fuel equivalence ratio δ_T. Uninstalled thrust is proportional to δ_T and increases as the Mach number increases; but the increasing speed decreases with the increase of Mach number. The specific fuel ratio also linearly varies with respect to δ_T, and increases with Mach number but decreases with altitude.

(4) As well as the thrust, lift force and pitch moment are generated at the forebody, which are part of the total aerodynamic force and momentum.

5. Modeling Results

5.1. AHV model

Data of aerodynamic characteristics and engine performance can be obtained from the preceding calculation. The data could be used by interpolation or fitting. Interpolation is suitable for small amount of but accurate sample data, such as the wind tunnel test data. Fitting is always employed in the situation emphasizing the approximate trends while the accuracy requirement is lower, such as the CFD calculation results. Hence, multivariate fitting is adopted and evaluated by relative error (RE). RE is defined as

$$\mathrm{RE}=\frac{\|\boldsymbol{u}-\hat{\boldsymbol{u}}\|}{\|\boldsymbol{u}\|}\times 100\% \tag{1}$$

where $\boldsymbol{u}$ is original data vector, $\hat{\boldsymbol{u}}$ the vector yield from fitting formula at the same state point, and $\|\bullet\|$ the norm of vector.

All the resultant fitting formulas are listed as follows:

$$\begin{aligned}C_{La}=C_{La}(Ma,\alpha,\delta_{e1},\delta_{e2})=\\ 0.149\,8-0.027\,51Ma+0.072\,35\alpha-\\ 0.003\,368\alpha Ma+0.002\,343Ma^2+\\ 0.001\,185\alpha^2+0.006\,515(\delta_{e1}+\delta_{e2})\end{aligned} \tag{2}$$

$$\begin{aligned}C_{Da}=C_{Da}(Ma,\alpha,\delta_{e1},\delta_{e2})=\\ 0.050\,99-0.004\,863Ma+0.002\,967\alpha+\\ 0.001\,364\alpha^2+0.000\,536\,27(\delta_{e1}+\delta_{e2})+\\ 0.000\,131\,3(\delta_{e1}^2+\delta_{e2}^2)\end{aligned} \tag{3}$$

$$\begin{aligned}C_Y=C_Y(Ma,\alpha,\beta,\delta_r)=\\ 0.046\,26\beta-0.002\,833\beta Ma-0.000\,369\,1\alpha\beta+\\ (-0.007\,779+0.000\,502\,69Ma)\delta_r\end{aligned} \tag{4}$$

$$\begin{aligned}C_l=C_l(Ma,\beta,\delta_r,\delta_{e1},\delta_{e2})=\\ (0.008\,739-0.000\,450\,27Ma)\beta+\\ (0.003\,319-0.000\,213\,96Ma)\delta_r+\\ (0.004\,906-0.000\,228\,31Ma)(\delta_{e1}-\delta_{e2})\end{aligned} \tag{5}$$

$$\begin{aligned}C_{ma}=C_{ma}(Ma,\alpha,\delta_{e1},\delta_{e2})=\\ 0.241\,4+0.011\,68Ma+\\ 0.101\,2\alpha+0.001\,21\alpha^2+\\ (-0.037\,02+0.001\,733Ma)(\delta_{e1}+\delta_{e2})\end{aligned} \tag{6}$$

$$\begin{aligned}C_n=C_n(Ma,\alpha,\beta,\delta_r,\delta_{e1},\delta_{e2})=\\ -0.001\,495\beta Ma-0.000\,286\,42\alpha\beta+\\ 0.012\,15\beta+(-0.012\,55+0.000\,981\,33Ma)\delta_r-\\ 0.000\,027\,973\delta_r^3-0.000\,078\,7(\delta_{e1}^2-\delta_{e2}^2)\end{aligned} \tag{7}$$

$$\begin{aligned}C_{Tc}=C_{Tc}(Ma,\alpha,\beta,\delta_T)=\\ 0.102\,9\delta_T-0.020\,22(Ma\cos\beta)\delta_T-\\ 0.001\,757\alpha\delta_T+0.000\,088\,233\alpha^2\delta_T+\\ 0.001\,221(Ma\cos\beta)^2\delta_T\end{aligned} \tag{8}$$

$$\begin{aligned}C_{Tn}=C_{Tn}(Ma,\alpha,\beta,\delta_T)=\\ 0.037\,91+0.005\,176\alpha-0.012\,35Ma\cos\beta-\\ 0.000\,548\,87(Ma\cos\beta)\alpha+\\ 0.000\,968\,97(Ma\cos\beta)^2+0.056\,27\delta_T-\\ 0.000\,774\,67\alpha\delta_T+0.002\,103(Ma\cos\beta)\delta_T\end{aligned} \tag{9}$$

$$\begin{aligned}C_{Le}=C_{Le}(Ma,\alpha,\beta,\delta_T)=\\ 0.721\,5+0.026\,35\alpha+0.114\,7Ma\cos\beta-\\ 0.002\,795(Ma\cos\beta)\alpha-0.578\,2(Ma\cos\beta)^{1/2}+\\ 0.289\,4\delta_T-0.004\,363\alpha\delta_T+\\ 0.010\,83(Ma\cos\beta)\delta_T\end{aligned} \tag{10}$$

$$\begin{aligned}C_{De}=C_{De}(Ma,\alpha,\beta,\delta_T)=\\ 0.002\,339\alpha+0.000\,121\,82\alpha^2-\\ 0.000\,331\,26(Ma\cos\beta)\alpha+0.005\,557\alpha\delta_T\end{aligned} \tag{11}$$

$$\begin{aligned}C_{me}=C_{me}(Ma,\alpha,\beta,\delta_T)=\\ -0.829\,7+0.270\,3Ma\cos\beta-0.113\,3\alpha-\\ 0.021\,21(Ma\cos\beta)^2+0.012\,01(Ma\cos\beta)\alpha-\\ 1.231\,5\delta_T+0.016\,95\alpha\delta_T-0.046\,02(Ma\cos\beta)\delta_T\end{aligned} \tag{12}$$

$$\begin{aligned}\frac{\dot{m}_f}{\delta_T}=\frac{\dot{m}_f(Ma,\alpha,\beta,H,\delta_T)}{\delta_T}=\\ 2.480\,5-0.054\,55\alpha+0.001\,599\alpha^2-0.204H+\\ 0.486Ma\cos\beta+0.002\,515\alpha H+0.003\,635H^2-\\ 0.008\,598(Ma\cos\beta)\alpha-0.012\,16(Ma\cos\beta)H\end{aligned} \tag{13}$$

where C_L, C_D and C_Y are coefficients of lift, drag and side forces, C_l, C_m and C_n are coefficients of rolling, pitching and yawing moments, C_T is coefficient of thrust, $\mathrm{d}m_f/\mathrm{d}t$ specific fuel consumption, subscript "a" means the aerodynamics calculation parts of the corresponding coefficients, "e" the engine calculation parts, "c" the combustor calculation parts, "n" the nozzle calculation parts.

The values of RE of all formulas are shown in Table 5. Fitting results can honestly reflect original data.

Table 5 RE of fitting results

Fitting variable	RE/%	Fitting variable	RE/%
C_{La}	4.91	C_{Le}	1.60
C_{Da}	5.45	C_{De}	2.56
C_Y	4.05	C_{me}	1.59
C_l	9.10	C_{Tc}	1.54
C_{ma}	7.31	C_{Tn}	1.59
C_n	8.59	$\mathrm{d}m_f/\mathrm{d}t$	5.81

Fitting results show that

(1) The lift, drag and pitching moment are affected by the propulsion system. Thus, they include aerodynamics part and propulsion part. Correspondingly the coefficients could be described as

$$C_L = C_{La} + C_{Le} \tag{14}$$

$$C_D = C_{Da} + C_{De} \tag{15}$$

$$C_m = C_{ma} + C_{me} \tag{16}$$

(2) The total thrust coefficient consists of uninstalled thrust coefficient and afterbody thrust coefficient, i.e.

$$C_T = C_{Tc} + C_{Tn} \tag{17}$$

(3) Because viscosity is not considered, altitude has no effect on aerodynamic coefficient and affects propulsion coefficient by within 2%. Therefore, the influence of altitude can be ignored. However, altitude still considerably influences fuel consumption (see Fig.6).

(4) As is consistent with the configuration, the attitude of AHV is changed by the following manners:

1) Rolling motion—differential movement of the two horizontal wings, that is $\delta_{e1}=-\delta_{e2}$.

2) Pitching motion—linkage movement of the two horizontal wings, that is $\delta_{e1}=\delta_{e2}$.

3) Yawing motion—BTT control method is adopted, that is $\delta_{e1}=-\delta_{e2}$ and $\delta_r\neq 0$.

In order to establish 6 DOF rigid-body model of AHV, equations of motion and geometric equations still need to be selected. For hypersonic flights, equations of motion are established reasonably with absence of wind and curved Earth without self-rotation[19-20]. All the equations are listed as follows.

Equations of motion are

$$\dot{V} = \frac{T\cos\alpha\cos\beta - D}{m} - \frac{G_M \sin\mu}{R^2} \tag{18}$$

$$\dot{\mu} = [T(\cos\alpha\sin\beta\sin\gamma + \sin\alpha\cos\gamma) + L\cos\gamma - Y\sin\gamma]/(mV) - [(G_M - V^2R)\cos\mu]/(VR^2) \tag{19}$$

$$\dot{\varphi} = [T(\sin\alpha\sin\gamma - \cos\alpha\sin\beta\cos\gamma) + L\sin\gamma + Y\cos\gamma]/(mV\cos\mu) + (V\cos\mu\tan\phi_{lat}\sin\varphi)/R \tag{20}$$

$$\dot{R} = V\sin\mu \tag{21}$$

$$\dot{\phi}_{long} = V\cos\mu\sin\varphi/(R\cos\phi_{lat}) \tag{22}$$

$$\dot{\phi}_{lat} = (V\cos\mu\cos\varphi)/R \tag{23}$$

$$\dot{p} = (c_1 r + c_2 p)q + c_3\bar{L} + c_4 N \tag{24}$$

$$\dot{q} = c_5 pr - c_6(p^2 - r^2) + c_7 M \tag{25}$$

$$\dot{r} = (c_8 p - c_2 r)q + c_4\bar{L} + c_9 N \tag{26}$$

$$\dot{\phi} = p + (r\cos\phi + q\sin\phi)\tan\theta \tag{27}$$

$$\dot{\theta} = q\cos\phi - r\sin\phi \tag{28}$$

$$\dot{\psi} = (r\cos\phi + q\sin\phi)/\cos\theta \tag{29}$$

where V is velocity; μ angle of track; φ yaw angle of track; γ roll angle of track; R distance between Earth center and vehicle centroid; ϕ_{long} and ϕ_{lat} are longitude and latitude; p, q and r roll, pitch and yaw rates; ϕ, θ and ψ roll, pitch and yaw angles; T is thrust; L, D and Y are lift, drag and side forces; $\bar{L}$, M and N are rolling, pitching and yawing moments; G_M is gravitational coefficient of Earth; c_1 to c_9 are constants related to the moment of inertia.

Geometric equations are

$$\sin\beta = [\cos\phi\sin(\varphi-\psi) + \sin\theta\sin\phi\cos(\varphi-\psi)]\cos\mu - \sin\mu\cos\theta\sin\phi \tag{30}$$

$$\sin\alpha\cos\beta = \cos\mu\sin\theta\cos\phi\cos(\varphi-\psi) - \cos\mu\sin\phi\sin(\varphi-\psi) - \sin\mu\cos\theta\cos\phi \tag{31}$$

$$\sin\gamma\cos\mu = \cos\alpha\sin\beta\sin\theta + \cos\theta\cos\beta\sin\phi - \cos\theta\sin\alpha\sin\beta\cos\phi \tag{32}$$

Atmosphere density and sound speed model[21] are

$$\rho = 0.003\,484\,p/T_{temp} \tag{33}$$

$$c = 20.05\sqrt{T_{temp}} \tag{34}$$

where ρ is atmospheric density, p atmospheric pressure, T_{temp} atmospheric temperature, c sound velocity.

Other equations are

$$Ma = V/c \tag{35}$$

$$R = R_E + H \tag{36}$$

$$L = \frac{1}{2}\rho V^2 S C_L \tag{37}$$

$$D = \frac{1}{2}\rho V^2 S C_D \tag{38}$$

$$Y = \frac{1}{2}\rho V^2 S C_Y \tag{39}$$

$$T = \frac{1}{2}\rho V^2 S C_T \tag{40}$$

$$\bar{L} = \frac{1}{2}\rho V^2 S b C_l \tag{41}$$

$$M = \frac{1}{2}\rho V^2 S c_A C_m \tag{42}$$

$$N = \frac{1}{2}\rho V^2 S b C_n \tag{43}$$

5.2. Trim flight simulation

Under the flight conditions of the given altitude, Mach number, longitude, and roll angle, trim flight simulation has been executed. The final trim result is shown in Fig.7. In Fig.7, q is the dynamic pressure and dQ the heating rate.

With the control variable limits and the angle of attack limit being considered, the two triangle marked boundaries are obtained. Since the scramjet is applied, there are two velocity limits ($V_{\min}$ and $V_{\max}$) to suit the property of scramjet. Besides, with dynamic pressure limit (the black boundary) and heating rate limit (the red boundary) being concerned, the whole flight corridor of AHV is acquired (see Fig.7). The state point (V, H) within the flight corridor indicates that

$$\delta_{e1,\min} \le \delta_{e1,\text{trim}} \le \delta_{e1,\max} \tag{44}$$

$$\delta_{e2,\min} \le \delta_{e2,\text{trim}} \le \delta_{e2,\max} \tag{45}$$

$$\delta_{T,\min} \le \delta_{T,\text{trim}} \le \delta_{T,\max} \tag{46}$$

$$\alpha_{\min} \le \alpha_{\text{trim}} \le \alpha_{\max} \tag{47}$$

$$V_{\min} \le V \le V_{\max} \tag{48}$$

$$q_{\text{trim}} \le 9\times10^4 \text{ Pa} \tag{49}$$

$$\mathrm{d}Q_{\text{trim}} \le 7.9\times10^5 \text{ W/m}^2 \tag{50}$$

where subscript "min" and "max" mean the corresponding limits; subscript "trim" means that the variable values are obtained from the trim calculation.

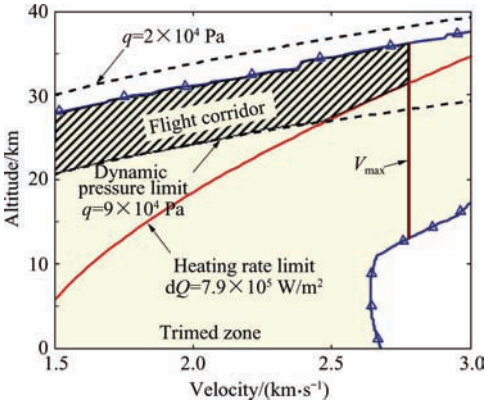

Fig.7 Flight corridor of AHV.

5.3. Model verification

The typical flight points of the similar vehicle are utilized to verify AHV model, since the general parameters and flight conditions are mainly referred to the vehicle (see Table 6).

Table 6 Typical flight points

Parameter	Point 1	Point 2	Point 3
V/(m·s^{-1})	1 788.2	1 812.7	1 963.8
H/km	24.4	24.4	30.5

Obviously, all the typical flight points are within the flight corridor of AHV, indicating that the Eqs.(44)-(50) are satisfied. Thus, the modeling of AHV is accomplished.

6. Conclusions

This article presents parameterized configuration approach for hypersonic vehicle modeling. Through parameterized aerodynamics/propulsion integration, inviscous hypersonic aerodynamic calculation and scramjet engine modeling, a 6 DOF rigid-body model of AHV is obtained. Trim results prove the rationality and effectiveness of AHV model.

Further work will be focused on model analysis, such as evaluating the impact of typical configuration parameters on the vehicle performance, analyzing vehicle's flight envelope and path constraints (angle of attack limit for scramjet, heating rate and dynamic pressure for body and wings, etc.).

References

[1] Zhang J M, Du X, Chen J. Development and prospect of nearspace vehicle technology. Nearspace Science & Engineering 2009; 1-6. [in Chinese]

[2] Shaughnessy J D, Pinckney S Z, McMinn J D, et al. Hypersonic vehicle simulation model: winged-cone configuration. NASA TM-102610, 1990.

[3] Keshmiri S, Colgren R, Mirmirani M. Development of an aerodynamic database for a generic hypersonic air vehicle. AIAA-2005-6257, 2005.

[4] Keshmiri S, Mirmirani M D. Six-DOF modeling and simulation of a generic hypersonic vehicle for conceptual design studies. AIAA-2004-4805, 2004.

[5] Keshmiri S, Colgren R, Mirmirani M. Six-DOF modeling and simulation of a generic hypersonic vehicle for control and navigation purposes. AIAA-2006-6694, 2006.

[6] Mirmirani M, Wu C, Clark A, et al. Modeling for control of a generic airbreathing hypersonic vehicle. AIAA-2005-6256, 2005.

[7] Clark A, Wu C, Mirmirani M, et al. Development of an airframe-propulsion integrated generic hypersonic vehicle model. AIAA-2006-218, 2006.

[8] Clark A D, Mirmirani M D, Wu C, et al. An aero-propulsion integrated elastic model of a generic airbreathing hypersonic vehicle. AIAA-2006-6560, 2006.

[9] Mirmirani M, Wu C, Clark A, et al. Airbreathing hypersonic flight vehicle modeling and control, review, challenges, and a CFD-based example. Workshop on Modeling and Control of Complex Systems. 2005; 1-15.

[10] Bolender M A, Doman D B. A non-linear model for the longitudinal dynamics of a hypersonic air-breathing vehicle. AIAA-2005-6255, 2005.

[11] Oppenheimer M W, Doman D B. A hypersonic vehicle model developed with piston theory. AIAA-2006-6637,

2006.
[12] Bolender M A, Doman D B. Nonlinear longitudinal dynamical model of an air-breathing hypersonic vehicle. Journal of Spacecraft and Rockets 2007; 44(2): 374-387.
[13] Rodriguez A A, Dickeson J J, Cifdaloz O, et al. Modeling and control of scramjet-powered hypersonic vehicles: challenges, trends, and tradeoffs. AIAA-2008-6793, 2008.
[14] Rodriguez A A, Dickeson J J, Sridharan S, et al. Control-relevant modeling, analysis, and design for scramjet-powered hypersonic vehicles. AIAA-2009-7287, 2009.
[15] He Y Y, Le J L, Ni H L. Numerical and experimental study of airbreathing hypersonic airframe/propulsion integrative vehicle. Journal of Experiments in Flulid Mechanics 2007; 21(2): 29-34. [in Chinese]
[16] Hank J M, Murphy J S, Mutzman R C. The X-51A scramjet engine flight demonstration program. AIAA-2008-2540, 2008.
[17] Che J. Optimization design of waverider-hypersonic cruise vehicle. PhD thesis, College of Astronautics, Northwestern Polytechnical University, 2006; 42-46. [in Chinese]
[18] Heiser W H, Pratt D T. Hypersonic airbreathing propulsion. Reston: AIAA, 1994; 175-192.
[19] Xiao Y L. Motion modeling of aeronautic and astronautical vehicle: theoretical foundation of flight dynamics. Beijing: Beijing University of Aeronautics and Astronautics Press, 2003; 38-50. [in Chinese]
[20] Wu S T, Fei Y H. Flight control system. Beijing: Beijing University of Aeronautics and Astronautics Press, 2005; 8-41. [in Chinese]
[21] National Oceanic and Atmospheric Administration, National Aeronautics and Space Administration, U.S. Air Force. U.S. standard atmosphere 1976. Washington, D.C: U.S. Government Printing Office, 1976; 12-23.

Biography:

LI Huifeng Born in 1970, she received B.S. and Ph.D. degrees from Xi'an Jiaotong University in 1991 and 1998 respectively, and is currently an associate professor of Beijing University of Aeronautics and Astronautics. Her main research fields are hypersonic vehicle guidance and control, and dynamic modeling.
E-mail: lihuifeng@buaa.edu.cn